Interlaminar Fracture Toughness of GFRP Influenced by Fiber Surface Treatment

R. Rikards, A. Korjakin, F. G. Buchholz, H. Wang, A. K. Bledzki and G. Wacker

Journal of Composite Materials 1998 32: 1528
DOI: 10.1177/002199839803201701

Interlaminar Fracture Toughness of GFRP Influenced by Fiber Surface Treatment

R. RIKARDS* AND A. KORJAKIN
Institute of Computer Analysis of Structures, Riga Technical University
LV-1658 Riga, Latvia

F.-G. BUCHHOLZ AND H. WANG**
Institute of Applied Mechanics
University of Paderborn
Pohlweg 47-49
D-33098 Paderborn, Germany

A. K. BLEDZKI AND G. WACKER
Institute of Material Science
University of Kassel
Mönchebergstr. 3, D-34109 Kassel, Germany

(Received November 24, 1996)
(Revised July 10, 1997)

ABSTRACT: The interlaminar fracture behavior of unidirectionally glass fiber reinforced composites with fiber surface treatments have been investigated in Mode I, Mode II and for a fixed mixed Mode I/II ratio. With respect to the loading conditions at the crack tip the double cantilever beam (DCB), the end notched flexure (ENF) and the mixed mode flexure (MMF) specimens were used in order to obtain Mode I, Mode II and mixed Mode I/II critical energy release rates. The data obtained from these tests have been analyzed by using analytical and finite element approaches. The present investigation is focused on the influence of the glass fiber surface treatment on the interlaminar fracture toughness. Glass fibers with two different fiber surface treatments have been investigated. For the DCB test the data reduction from the experiments have been carried out by using six different approaches: the area method, the Berry method, the modified beam analysis, the compliance method and the geometric linear and non-linear finite element analysis. The geometric non-linear finite element analysis of the DCB test was performed firstly. For the ENF test contact and friction along the crack surfaces have been taken into account.

*Author to whom correspondence should be addressed.
**DAAD PhD scholarship fellow from Harbin Engineering University, Harbin, PR China.

0021-9983/98/17 1528–32 $10.00/0

KEY WORDS: composites, interlaminar fracture toughness, Mode I, Mode II, mixed Mode I/II.

1. INTRODUCTION

ONE OF THE major disadvantages of laminated composites is their tendency to delaminate. In composites containing brittle matrices, delamination can propagate even more readily compared to transverse cracks that are perpendicular to the plane of the laminate. Initiation and growth of delamination can reduce considerably the stiffness and compressive strength of composites.

Macroscopic properties of fiber reinforced composites are dependent on the micro mechanics of the fiber/matrix interphase. Therefore, the adhesion between fibers and matrix is very important for the mechanical behavior of fiber reinforced laminated polymeric composites.

There are several test methods to determine the fiber/matrix adhesion properties. Widely used are such experimental methods as fiber pull-out, fragmentation, microtension and microcompression tests [1]. From macro test methods the fiber/matrix adhesion properties can only be obtained indirectly. For example, such tests are the transverse tension or interlaminar shear experiments. Information about the fiber/matrix adhesion can also be obtained from experiments on the propagation behavior of delamination cracks. These experiments are used in the present investigation.

The significant role of delamination in the fracture of composites is reflected by the large number of papers published in this field [2–17]. In these investigations delamination or interlaminar fracture toughness properties of different fiber reinforced composites were investigated. Mode I, Mode II, Mode III and mixed mode loading conditions were used to determine the corresponding critical energy release rates or fracture toughness.

There are a number of investigations concerned with the measurement of the Mode I interlaminar fracture toughness in composite materials [3–5,7,9,11] [14,15,17–19]. Mode I (crack opening) loading conditions are used as a basic test to evaluate the fiber/matrix adhesion properties of a composite. The double cantilever beam (DCB) type configuration is one of the most common specimen geometries to determine the critical energy release rate G_{IC}. The advantage of the DCB test is simple specimen geometry and the stable crack growth.

Mode II (crack sliding or in-plane shear) loading conditions are used for the evaluation of the critical energy release rate G_{IIC} [20]. For this the end notched flexure (ENF) specimen is commonly used [3,7,12,14,16,21]. The advantage of the ENF test is the simple three point bending specimen geometry. The disadvantage is the unstable crack growth and some influence of friction along the crack surfaces adjacent to the support. Therefore, by using the ENF test the critical energy release rate G_{IIC}^{init} can be determined only for crack initiation. In this case the

critical energy release rates for crack propagation have to be obtained from other tests. Mode II loading conditions also can be achieved by using end loaded split (ELS) specimens [3,7]. In this case the lower arm of the ELS specimen is loaded. In general in the ELS test unstable crack growth will occur, however, for certain ratios of initial crack length also stable crack growth can be achieved. Similar to the ENF specimen is the so called center notch flexural (CNF) test specimen [22], which also can be used to obtain the Mode II critical energy release rate.

Mixed Mode I/II tests are characterized by the ratio G_I/G_{II} that is driving the crack. Various mixed mode ratios G_I/G_{II} can be obtained by using different specimens. The mixed mode flexure (MMF) test is Mode I dominated with a ratio of $G_I/G_{II} = 1.33$ obtained from linear beam analysis [3]. This ratio is valid, when upper and lower parts of the specimen are of equal thickness [3]. By varying the thickness ratio of the lower and upper parts different mixed Mode I/II ratios can be obtained. However, as it will be shown below for the MMF specimen, the mixed mode ratio obtained by the finite element solution is dependent on crack length and in the case of equal thickness of lower and upper parts is varying from 1.4 to 1.5. In the case when the ELS specimen is loaded by the upper arm mixed mode loading conditions at the crack tip are achieved. For a symmetrical geometry the mixed Mode I/II ratio obtained from the linear beam analysis is $G_I/G_{II} = 1.33$ [7].

For mixed mode tests also other specimens can be used. Very similar to the MMF specimen is the so called single leg bending (SLB) specimen [10] for which only the supports are of different height. With this specimen also different mixed Mode I/II ratios can be achieved, but Mode I remains dominant. By the crack lap shear (CLS) test also various G_I/G_{II} ratios can be achieved through varying the stepped thickness ratio, however, in this case Mode II is dominant [3]. The crack growth for the CLS test is semi-stable and it is possible to record several data points with crack growth. However, for these test measurements suffer from large scatter with increasing of crack length [3]. Mixed mode loading conditions can be generated also by using the edge delamination tension (EDT) specimen [23].

For all mixed mode specimens discussed above there are limited possibilities to achieve a wide range of mixed mode ratios. By loading the ENF specimen with a special loading lever different mixed mode ratios can be achieved. This is the so called mixed mode bending (MMB) test, which was proposed in [13]. The MMB test simply combines the Mode I DCB and the Mode II ENF tests and by different loading positions various mixed mode ratios are achieved. In paper [13] the experiments were carried out with G_I/G_{II} ratios from 0.25 to 4, whereas in [24] the G_I/G_{II} ratios vary even from 0.002 to 35. Now the MMB specimen is widely used to determine mixed mode critical energy release rates for different composites [6,13,24].

However, as may be seen from the data reported in the literature, the values of

critical energy release rates are frequently dependent on the method of analysis employed for the data reduction. For example, it has been observed that the area and the compliance calibration method, which are two direct approaches for the calculation of critical energy release rates, may give different values compared to those obtained by using the linear beam theory. In papers [7,8,18] corrections in the formulae based on the linear beam theory were proposed by taking into consideration such effects as the end rotation and deflection of the crack tip, the effective shortening of the beam due to large displacements and the stiffening of the beam due to the presence of the end blocks bonded to the specimens.

For the end notched flexure (ENF) specimen the influence of friction at the crack surfaces was evaluated [12,20] and it was found that for this case in the balance of energy the work of friction is only to the amount of 2% to 4%. So, the calculations by using simple analytical formulae based on beam theory can be performed also for ENF specimens, but more exact solutions have been obtained by using the finite element method [25].

One way to improve the delamination fracture toughness of composites is focused on improving the fracture toughness of the matrix by using toughened resin systems or thermoplastic matrices [2,14]. However, an increase in resin toughness is not completely realized in interlaminar fracture toughness of composites having poor adhesion between fibers and matrix. Interlaminar fracture toughness is highly dependent on fiber/matrix adhesion. Therefore, another way to increase the interlaminar fracture toughness of a composite is to improve the fiber/matrix adhesion by fiber surface treatments, which changes the fiber surface morphology and chemistry.

There are different methods available for fiber surface treatments of carbon [26] and aramid [27] fibers. Increasing the level of adhesion in the fiber/matrix interface yields significant improvements in the interlaminar fracture toughness [16]. In the present paper composites reinforced by glass fibers with surface treatments are investigated. Although glass fibers with surface treatment have been used for a long time the fiber/matrix interface morphology and chemistry are not completely understood [28]. How to improve the glass fiber adhesion with the matrix by using coupling agents was discussed widely in the literature [29–31]. The surface of the glass fibers used in the present investigation were improved by a technology, which was outlined previously [32].

The goal of this investigation is to study the influence of the fiber surface treatment on the interlaminar fracture toughness and to evaluate the various methods of analysis of experimental data. Delamination of unidirectional glass/epoxy laminates under Mode I, Mode II and mixed Mode I/II loading conditions is investigated. In the present investigation for Mode I tests DCB specimens are used, for Mode II tests ENF specimens are used and for mixed Mode I/II tests MMF specimens are used. The data reduction from experiments for the DCB test have been carried out by using six different approaches: the area method, the Berry method,

the modified beam analysis, the compliance method and the linear and geometric non-linear finite element analysis. For the ENF and MMF tests only the data reduction by using the beam analysis and the linear finite element analysis were considered to be sufficient. For the ENF test contact and friction along the crack surfaces have been taken into account. In the case of friction a separated critical energy release rates G_I and G_{II} are calculated by using the virtual crack closure integral (VCCI) method.

2. MATERIAL

For the production of the composite material to be considered in this investigation borosilicate glass fibers (E-glass) with small parts of alkali and a brittle epoxy matrix (Araldite LY 556 with curing agent Hy 917, Ciba Geigy Ltd.) were used. For the fibers embedded in the brittle epoxy matrix two different types of fiber surface treatments were chosen. The first type of sizing (surface treatment SI/EP) is based on using a silane coupling agent (Aminosilane 1100) in a mixture with an epoxy modifying agent [33]. The second type of sizing (surface treatment PE) is based on a modification of the fiber surface with polyethylene.

Unidirectionally reinforced glass fiber plates were produced through winding

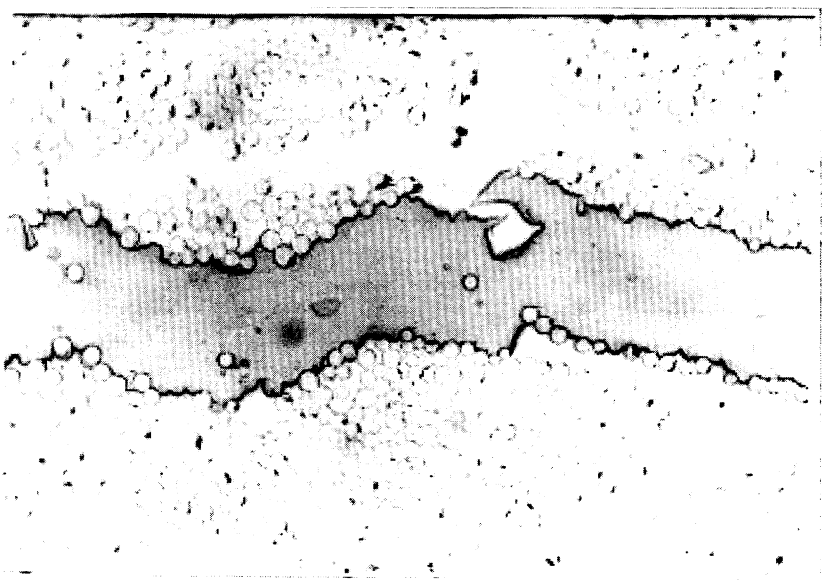

Figure 1. *View of the Mode II delamination crack perpendicular to the beam axis for the composite PE (magnification 200:1).*

technology. The plates contained a starter crack, which was introduced by a Teflon film (thickness 40 μm) placed between the central plies. The total number of plies was 12 in order to get a plate thickness of approximately 3 mm. The laminates were produced by following the standard cure cycle recommended by Ciba Geigy Ltd. In order to improve the quality of the plates and to reduce the void content, the plates were placed in a vacuum before curing. The specimens were cut with a diamond wheel and kept at room temperature until testing (23°C and 50% of relative humidity). All tests were performed at the same conditions. For both composites (SI/EP and PE) the fiber volume content of the specimens was 50% (±1.2%). In Figure 1 the micro structure of the UD fiber reinforced composite can be observed. In the production of these composite by the filament winding technology the 60 TEX roving have been used with 204 fibers in one roving. It is seen that due to the filament winding technique the distribution of the fibers in the cross section is irregular and large areas of the pure matrix material between the rovings can be observed. However, in calculations the composite is considered to be a homogeneous transversal isotropic material.

The elastic properties of the composites investigated in this paper are as follows. For the SI/EP composite the modulus of elasticity in the fiber direction (longitudinal modulus) is $E_1 = 40700$ MPa and the transverse modulus is $E_2 = 10269$ MPa. For the PE composite the corresponding values are slightly lower: $E_1 = 39760$ MPa and $E_2 = 7449$ MPa. Here the axis 1 is in the fiber direction and axis 2, 3 are in the transverse directions. These properties were obtained from tension tests [33]. For the longitudinal modulus E_1 the values obtained by data reduction from the DCB tests (see below) are in good agreement with those obtained from the tension test.

In the same tension experiments the transverse interlaminar strength properties were determined [33]. For the SI/EP composite the transverse tension strength is found to be $R_2^+ = 58.1$ MPa, whereas for the PE composite the transverse interlaminar strength in tension is about 3 times lower: $R_2^+ = 18.4$ MPa. So, in the case of interlaminar tension the fiber/matrix adhesion properties for the PE composite is poor in comparison with the SI/EP composite. The modulus of elasticity of the brittle epoxy resin used for the production of the composites is $E_m = 3110$ MPa, Poisson's ratio is $\nu_m = 0.34$ and the ultimate strain at failure is 3.3% [33].

The other elastic properties for the UD fiber reinforced composite with a fiber volume content of 50% were obtained by using the analytical expressions in order to calculate the effective stiffness of the material [34]. In these calculations the modulus of elasticity of the fibers is considered to be $E_f = 78000$ MPa and Poisson's ratio is $\nu_f = 0.20$. The following effective elastic properties were obtained: for the shear modulus $G_{12} = G_{13} = 4200$ MPa, for the shear modulus in the plane of isotropy $G_{23} = 3980$ MPa and for the Poisson's ratio in the same plane $\nu_{23} = 0.29$. These properties are used for the calculation of the correction coefficients (see below) and for the two dimensional (2D) finite element analysis.

3. TEST SPECIMENS AND EXPERIMENTAL PROCEDURE

3.1 Mode I Double Cantilever Beam (DCB) Specimen

The double cantilever beam (DCB) was used for those test in which Mode I loading conditions at the crack front had to be achieved. The DCB specimen is shown in Figure 2 for which the dimensions have been chosen as recommended in the literature [35].

Precracks of length $a_p - a_0 = 2.5$ mm were introduced into the specimens by a starter film of length $a_0 = 31$ mm. The loads were applied to the specimen via pins through universal joints and aluminium blocks that were bonded on the specimen.

For the experiments the testing machine Zwick 1446 was used. The loading was realized through a given displacement rate 1.0 mm/min^{-1}. The specimen was loaded until a quasi-static crack extension of approximately 10 mm was observed and then it was unloaded. This procedure was repeated until the crack had reached a final length of about 100 to 120 mm. The crack opening displacement (COD) δ on the load line was measured from the displacement of the testing ma-

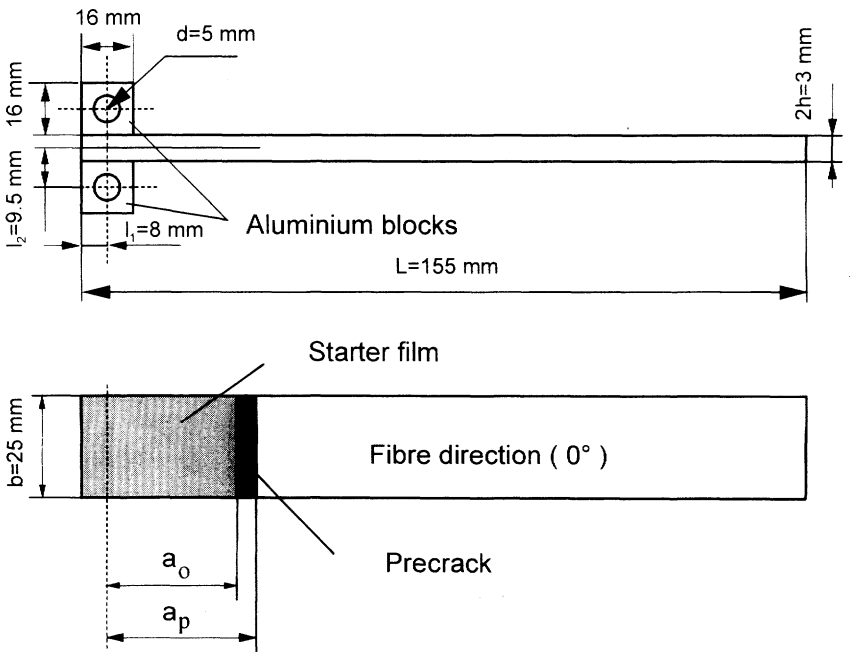

Figure 2. *Double cantilever beam specimen (DCB) for the Mode I tests and dimensions of the specimen and the aluminium blocks (in mm).*

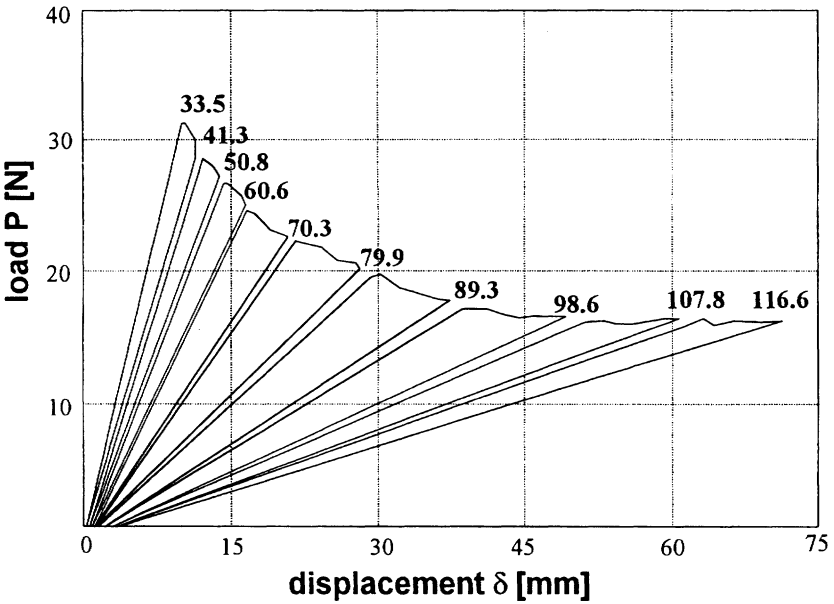

Figure 3. *Typical load* P *against displacement* δ *diagram in the DCB test for composite SI/EP. Crack lengths* a *(mm) are presented for the critical values of the load.*

chine. A typical load crack opening displacement diagram as function of crack length is shown in Figure 3. It can be seen that UD laminates show stable crack growth under Mode I loading conditions of the DCB test even for a brittle epoxy matrix.

3.2 Mode II End Notched Flexure (ENF) Specimen

The Mode II tests were performed by the aid of end notched flexure (ENF) specimen (see Figure 4), and a three point bending fixture with a span distance of $2L = 76$ mm and a width of the specimen of $b = 25$ mm, i.e., the same as for the DCB specimen. The thickness of the specimen is $2h = 3$ mm and it contains a symmetric split. Precracks of length from 4 mm to 10 mm were introduced before testing by loading with the crack opening mode, so that the initial position of the crack tip was at one fourth of the span of the beam. The loading during the test was carried out again by a given displacement rate of 1.0 mm/min^{-1}. When the limit load was reached, unstable crack growth occurred until crack arrest in the mid-span below the compression load. The limit load P and the critical displacement δ (deflection) at the mid-span of the beam were measured at the beginning of the crack extension.

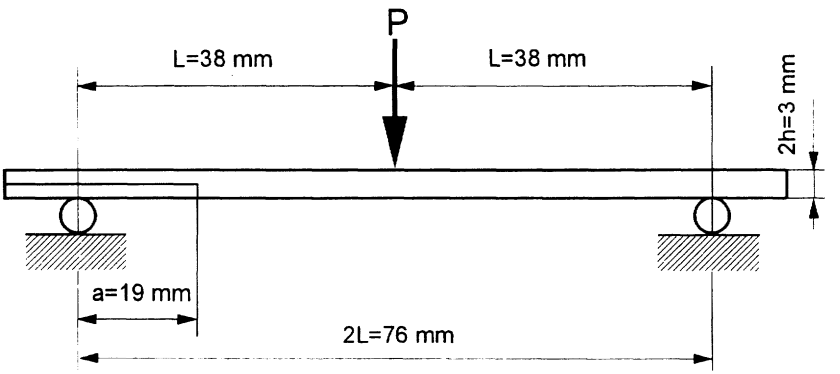

Figure 4. *End notched flexure specimen (ENF) for the pure Mode II tests.*

3.3 Mixed Mode Flexure Specimen (MMF) for the Mixed Mode I/II Tests

Mixed Mode I/II tests were performed by using the MMF specimen (see Figure 5). The thickness of the specimen is again $2h = 3$ mm with a symmetric split and the width of the specimen is $b = 25$ mm, i.e., the same as for the DCB and ENF specimens. Precracks of length from 3 mm to 5 mm were introduced before testing by Mode I loading so that the initial position of the crack tip was again at one fourth of the span of the beam. For this specimen Mode I is dominating at the crack tip. The mixed Mode I/II ratio for the MMF specimen with a symmetric split is $G_I/G_{II} = 1.33$ according to linear beam analysis, but by the finite element analysis ratios between 1.4 and 1.5 are found depending on crack length. The displacement rate during loading was 1.0 mm/min^{-1} and again test procedure with unloading was used, since in this case stable crack growth was observed again. This specimen was loaded until a quasi-static crack extension of approximately 5 mm was observed

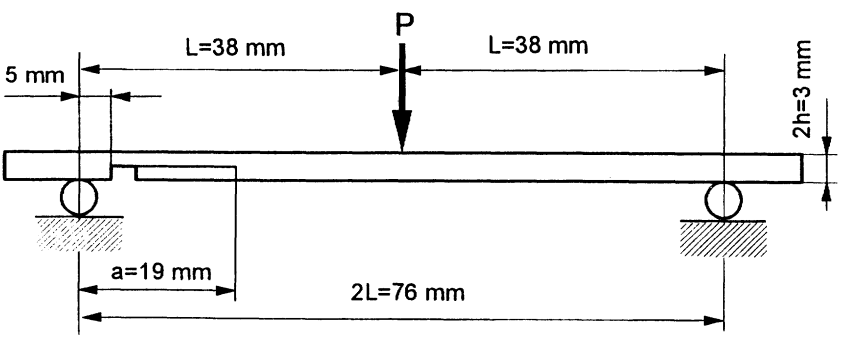

Figure 5. *MIxed mode flexure (MMF) specimen for the mixed Mode I/II tests.*

and then unloading was enforced. This procedure was repeated until crack extension till the mid-span of the beam, while critical loads P and corresponding deflections at the mid-span measured.

It should be mentioned that for all test specimens (DCB, ENF, MMF) the fibers of the UD reinforced composite were in the direction of the beam axis.

4. CALCULATION OF THE INTERLAMINAR FRACTURE ENERGIES

4.1 Area Method

A direct method for the evaluation of the total energy release rate is the area method. According to this method the released energy due to crack extension can be calculated by using Irwin's formula for the critical energy release rate

$$G_{TC} = -\frac{1}{b}\frac{\partial \Pi}{\partial a} \tag{1}$$

where $\Pi = U - W$ is the total potential of the structure, U is the strain energy, W is the work of the external forces (dead loads) and b and a are the width and crack length, respectively. In the case of linear elastic behavior of the structure $\Pi = -U$ is holding for the total potential. This means that the change in U due to crack extension from a to $a + \Delta a$ is simply the area between the loading and unloading curves in Figure 2. For an elastic body $\Pi = -U$ is substituted in formula (1) and thus the critical energy release rate is given by formula

$$G_{TC} = \frac{\Delta U}{b\Delta a}$$

$$\Delta U = \frac{1}{2}(P_1\delta_2 - P_2\delta_1) \tag{2}$$

Here P_1 and δ_1 are the load and displacement at crack length a and P_2 and δ_2 are the respective values at crack length $a + \Delta a$. Formula (2) can be used to calculate the critical energy release rates for Mode I, Mode II or mixed Mode I/II loading conditions. However, in the case of mixed mode conditions by Equation (2) only the total energy release rate G_{TC} can be calculated. In this case the separate energy release rates only can be calculated if from another solution the Mode I and Mode II values can be determined separately.

4.2 Compliance Method

Since the strain energy for linear response is $U = P\delta/2$ and $\Pi = -U$, the energy release rate in Equation (1) can be expressed through the compliance [36]

$$G_{IC} = -\frac{1}{b}\frac{\partial \Pi}{\partial a} = \frac{1}{b}\frac{\partial U}{\partial a} = \frac{P^2}{2b}\frac{\partial C}{\partial a} = \frac{P\delta}{2bC}\frac{\partial C}{\partial a} \tag{3}$$

where P is the critical load at which crack growth is observed, $C = \delta/P$ is the compliance, δ is the displacement and a is the crack length. In order to evaluate G_{IC} the compliance must be calculated by using experimental data, i.e., the measurements of loads and displacements at different crack length. The approximation of the function $C = C(a)$ for the composites investigated in the present paper will be shown below. The curve fit for the compliance must be performed with great accuracy, since in formula (3) the first derivative of the compliance function determines about the precision of the calculated critical energy release rate.

4.3 Linear Beam Analysis

4.3.1 BERRY METHOD FOR DCB TEST

For the DCB specimen the compliance calculated by the linear beam theory is given by [36]

$$C = \frac{\delta}{P} = \frac{8a^3}{bh^3E_1} \tag{4}$$

Here E_1 is the modulus of elasticity in the direction of the beam axis. Since the DCB specimen is relatively thin, the transverse shear effects can be neglected. From formula (4) the longitudinal modulus E_1 can be calculated by using the data of experiments from the DCB test

$$E_1 = \frac{P}{\delta}\frac{8a^3}{bh^3} \tag{5}$$

By substituting expression (4) into formula (3) the critical Mode I energy release rate for the DCB test can be calculated through

$$G_{IC} = \frac{3P\delta}{2ba} \tag{6}$$

and with δ substituted again from Equation (4) through

$$G_{IC} = \frac{12P^2a^2}{b^2h^3E_1} \tag{7}$$

If the data reduction is applied together with the least square technique [16] formula (6) can be used for the determination of the mean value of G_{IC}. However, the coefficient 3, obtained by the classical beam theory can be corrected by using the data of experiments. Such a method was proposed by Berry in 1963 [37]. In this case Equation (6) is rewritten by introducing an unknown quantity n

$$G_{IC} = \frac{nP\delta}{2ba} = \frac{nP^2C}{2ba} \tag{8}$$

According to beam theory the parameter n should be 3, but from the experimental data this unknown quantity n can be determined from

$$C = A_1a^n \tag{9}$$

Because in logarithmic coordinates Equation (9) can be written as

$$\lg C = \lg A_1 + n \lg a \tag{10}$$

Equation (10) can be used in order to determine A_1 and n by the least square method. As input data the experimental values C and a at the critical load P of each step of crack propagation for all specimens are used. The approximation of the experimental data by using the Berry method will be shown below.

4.3.2 ENF TEST

For the Mode II ENF test the compliance calculated by linear beam theory is given through [7,8,20]

$$C = \frac{3a^3 + 2L^3}{8E_1bh^3} \tag{11}$$

By substituting this expression into Equation (3) the critical energy release rate for the ENF test can be obtained from

$$G_{IIC} = \frac{9Pa^2\delta}{2b(3a^3 + 2L^3)} \tag{12}$$

4.3.3 MMF TEST

In a similar way for the Mode I/II MMF test the compliance can also be calculated by linear beam theory through [3]

$$C = \frac{1}{64E_1bh^3}(121L^3 + 448a^3) \tag{13}$$

By substituting expression (13) into Equation (3) the total critical energy release rate for the MMF test can be obtained from

$$G_{TC} = G_I + G_{II} = \frac{672a^2P\delta}{b(121L^3 + 448a^3)} \tag{14}$$

Because for the MMF test a fixed mixed Mode I/II ratio of $G_I/G_{II} = 1.33$ follows from linear beam analysis, here also the separated critical energy release rates can be obtained with

$$G_{IC} = 0.57G_{TC}; G_{IIC} = 0.43G_{TC} \tag{15}$$

It will be shown below that by the finite element analysis for the MMF test the mixed Mode I/II ratios between 1.4 and 1.5 are found depending on crack length.

4.4 Modified Beam Analysis

It was observed that different data reduction methods result in different values of the critical energy rates. This is because in linear beam theory some effects are not taken into account [7,8]. These effects are the rotation and deflection at the crack tip, the large displacements occurring in some of the test specimen and stiffening effects due to the presence of the bonded end blocks. In order to take these effects into account some correction coefficients were introduced [7,8], with which the data reduction formulae of the linear beam theory can be corrected for all specimens. In the following these modified beam analysis formulae will be outlined briefly.

For the DCB, ENF and MMF specimens the rotation effect at crack tip can be accounted for by adding a length χh to the measured crack length a. The coefficient χ can be calculated by the elastic properties of the material [7,8]

$$\chi = k_1\sqrt{\frac{E_1}{G_{13}}}\left[3 - 2\left(\frac{\Gamma}{\Gamma + 1}\right)^2\right]^{1/2} \tag{16}$$

with

$$\Gamma = \frac{1.18}{G_{13}}\sqrt{\frac{E_1}{E_2}}$$

In formula (16) for the DCB test it is recommended to choose $k_1 = \sqrt{1/11} = 0.302$ [7,8], and for the ENF test $k_1 = \sqrt{1/63} = 0.126$ is recommended [25]. In this way the corrected crack length was obtained also for the ENF test, for which subsequently the critical energy release rate G_{IIC} was calculated by the modified beam analysis. The comparison with G_{IIC} results obtained by the finite element method [25] show good agreement of both results.

Another correction factor F can be introduced to take the large displacements into account [7,8]

$$F = 1 - \Theta_1\left(\frac{\delta}{L}\right)^2 - \Theta_2\left(\frac{\delta l_1}{L^2}\right) \tag{17}$$

Here for the Mode I DCB test $\Theta_1 = 3/10, \Theta_2 = 3/2$ was given in [8] and l_1 is defined in Figure 2. For the ENF test the expression for Θ_1 was also given in [8]. Since in the ENF specimen there are no end blocks the coefficient $\Theta_2 = 0$.

In addition for the DCB specimen a correction factor N is required to account for the stiffening effect caused by the end blocks [7,8]

$$N = 1 - \Theta_3\left(\frac{l_2}{L}\right)^3 - \Theta_4\left(\frac{\delta l_1}{L^2}\right) - \Theta_5\left(\frac{\delta}{L}\right)^2 \tag{18}$$

Here l_2 is defined in Figure 1 and the additional coefficients for the DCB specimen are given in Reference [8]

$$\Theta_3 = 1, \Theta_4 = \frac{9}{8}\left[1 - \left(\frac{l_2}{L}\right)^2\right], \Theta_5 = \frac{9}{35} \tag{19}$$

The coefficient N is required in order to correct the measured values of displacement δ, which are to be used for the calculations of the compliance C, the modulus E_1 and the delamination energy G_{IC}.

The modified beam analysis formulae containing the discussed corrections for all specimens under consideration are given below.

4.4.1 MODE I TEST BY DCB SPECIMEN

For the DCB specimen the Equations (4–7) are corrected as follows [7,8]

$$C = \frac{8N(a + \chi h)^3}{bh^3 E_1} \tag{20}$$

$$\left(\frac{C}{N}\right)^{1/3} = (a + \chi h)\sqrt[3]{\frac{8}{bh^3 E_1}} \tag{21}$$

$$G_{IC} = \frac{F}{N}\frac{3P\delta}{2b(a + \chi h)} \tag{22}$$

$$G_{IC} = \frac{12FP^2(a + \chi h)^2}{b^2 h^3 E_1} \tag{23}$$

$$E_1 = \frac{P}{\delta}\frac{8N(a + \delta h)^3}{bh^3} \tag{24}$$

4.4.2 MODE II TEST BY ENF SPECIMEN

For the ENF specimen Equations (11) and (12) are corrected as follows [7,8]

$$C = \frac{3(a + \chi h)^3 + 2L^3}{8E_1 bh^3} \tag{25}$$

$$G_{IIC} = F\frac{9P(a + \chi h)^2\delta}{2b[3(a + \chi h)^3 + 2L^3]} \tag{26}$$

4.4.3 MIXED MODE I/II TEST BY MMF SPECIMEN

For the MMF specimen the Equations (13) and (14) also can be corrected

$$C = \frac{1}{64E_1 bh^3}[121L^3 + 448(a + \chi h)^3] \tag{27}$$

$$G_{TC} = G_1 + G_{II} = F\frac{672(a + \chi h)^2 P\delta}{b[121L^3 + 448(a + \chi h)^3]} \tag{28}$$

It should be mentioned that for all specimens the crack length correction term χh can be obtained not only by formula (16) but also directly from experimental data by using a curve fit procedure for the compliance C versus crack length a, which will be discussed below.

4.5 Finite Element Analysis

The finite element analysis of the experimental tests is performed by using the program ABAQUS [38] for plane strain conditions and with standard four-node quadrilateral elements. It was shown [39,40] that by using the modified virtual crack closure integral (MVCCI) method in combination with standard elements also good results for energy release rates can be obtained in comparison with higher order elements or reference solutions. Here $\Delta a = 0.2$ mm is taken for the values of successive crack extensions, which is coinciding with the finite element length along the crack.

For the calculation of the energy release rates G_I and G_{II} in the case of traction free crack surfaces (without contact and friction) the MVCCI method is used. Then the separated strain energy release rates are obtained by only one calculation (MVCCI or 1C method) for the actual crack length a as proposed in [39] (see Figure 6)

$$G_I^{1C}(a) = \frac{1}{b\Delta a} \cdot \frac{1}{2}\left[F_y^i(a)\Delta u_y^{i-1}(a)\right];$$

$$G_{II}^{1C}(a) = \frac{1}{b\Delta a} \cdot \frac{1}{2}\left[F_x^i(a)\Delta u_x^{i-1}(a)\right] \tag{29}$$

where $F_x^i(a)$ and $F_y^i(a)$ are the nodal point forces at the crack tip node i in x and y directions, respectively, while $\Delta u_x^{i-1}(a)$ and $\Delta u_y^{i-1}(a)$ are the relative nodal point displacements of the opposite crack faces at node i-1 in x and y directions, respectively. Therefore $\Delta u_x^{i-1}(a)$ is the crack sliding displacement, while $\Delta u_y^{i-1}(a)$ is the crack opening displacement at a distance Δa behind the crack tip.

In the case of the ENF test contact and friction along the crack surfaces has to be considered in the region of the support (see Figure 4). In this case the global potential energy of the beam is

$$\Pi = U - W + W^D \tag{30}$$

with U for the elastic strain energy of the beam, $W^D \equiv W^F$ for the energy dissipated due to friction at the crack faces and W for the work of the external forces. The dissipated energy is equal to the frictional work W^F performed at the crack surfaces, where Coulomb's friction law is used

$$C_x = \mu C_y \tag{31}$$

Here μ is the coefficient of friction, C_x is the frictional force and C_y is the contact

force at correlated nodal points on the crack faces [41]. They correspond to the nodal point forces F_x and F_y at the crack tip in formula (29). But a different notation is used for all nodes behind the crack tip, that means along the crack surfaces which may open or may be in sliding contact. At the crack faces contact elements [38] are used. In the case of contact and friction along the crack surfaces the frictional work is calculated by [41]

$$W_{ij}^{F} = \frac{1}{2} C_x^{j-1}(a + \Delta a)\Delta u_x^{j-1}(a + \Delta a) + \sum_{\kappa=1}^{j-1} \frac{1}{2} \left[C_x^{i-k}(a) + C_x^{j-(1+k)}(a + \Delta a)\right]\left[\Delta u_x^{j-(1+k)}(a + \Delta a) - \Delta u_x^{i-k}(a)\right] \tag{32}$$

Formulae (30) and (32) are used to calculate the total energy release rate

$$G_T^{EN2}(a) = -\frac{\Pi(a + \Delta a) - \Pi(a)}{b2\Delta a} \tag{33}$$

In the case of contact and friction along crack surfaces instead of MVCCI method the separated energy release rates must be calculated by the virtual crack closure integral method (VCCI or 2C method; see Figure 6)

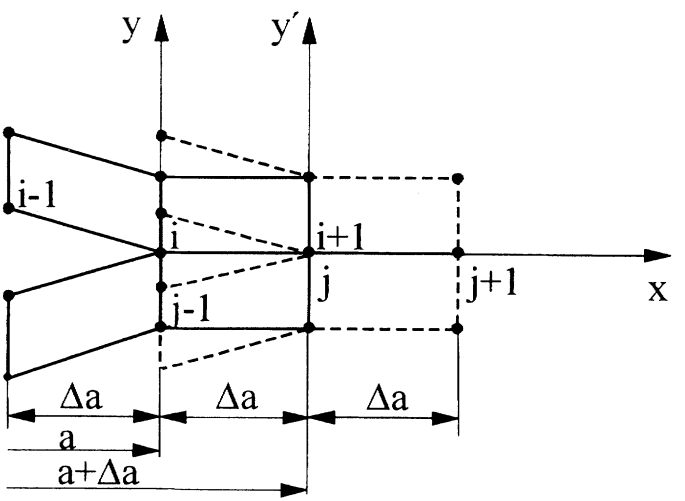

Figure 6. *Finite element mesh and nodal point notation near the crack tip.*

$$G_T^{2C}\left(a+\frac{\Delta a}{2}\right)=\frac{1}{b\Delta a}\cdot\frac{1}{2}\left[F_y^i(a)\Delta u_y^{j-1}(a+\Delta a)\right];$$
$$G_{II}^{2C}\left(a+\frac{\Delta a}{2}\right)=\frac{1}{b\Delta a}\cdot\frac{1}{2}\left[F_x^i(a)\Delta u_x^{j-1}(a+\Delta a)\right] \tag{34}$$

In the formulae (34) the nodal forces are calculated for the crack length a, while the displacements are taken for the crack length $a + \Delta a$. Therefore the energy release rates in formulae (34) are exact mean values for the crack length $a + \Delta a/2$and a finite crack extension Δa. The formulae (34) have been used also in the case of traction free crack surfaces (for DCB and MMF specimens). In this case both methods (VCCI and MVCCI) gives about the same results of the energy release rates.

Therefore, the total energy release rate $G_T = G_I + G_{II}$ of the specimen can be calculated from the separated energy release rates (29) or (34), or from the formula (33).

5. RESULTS FOR CRITICAL ENERGY RELEASE RATES

The critical energy release rates G_{IC} and G_{IIC} are calculated from the data of the experiments by the aid of different data reduction formulae, which were presented in the previous section. The data reduction for the Mode I test by using the DCB specimen is performed by six various approaches: the area method, the compliance method, the Berry method, the modified beam analysis and in addition by the linear and geometric non-linear finite element analysis. The data reduction for the Mode II ENF test are carried out by linear beam analysis and by finite element analysis taking into account the contact and friction along the crack surfaces. The data reduction for the mixed Mode I/II MMF test is also performed by linear beam analysis and by linear finite element analysis.

5.1 Mode I DCB Test

In the Mode I DCB test 10 steps of crack extension were measured. For the composite SI/EP the experiments on the delamination crack propagation were performed for 9 specimens, whereas for the composite PE 10 specimens have been available. For these tests the crack growth was carefully controlled so that at each step the values of crack length a were about the same for all specimens. Therefore, the critical loads and the corresponding crack opening displacements can be averaged for each step from the data obtained from all specimens. The scatter and the 95% confidence limits of the critical load for the composite PE is shown in Figure 7. The corresponding mean values of the load P, the crack length a and the displacement δ for the composites SI/EP and PE are presented in Table 1.

By using the experimental data of the DCB tests the calculation of the critical

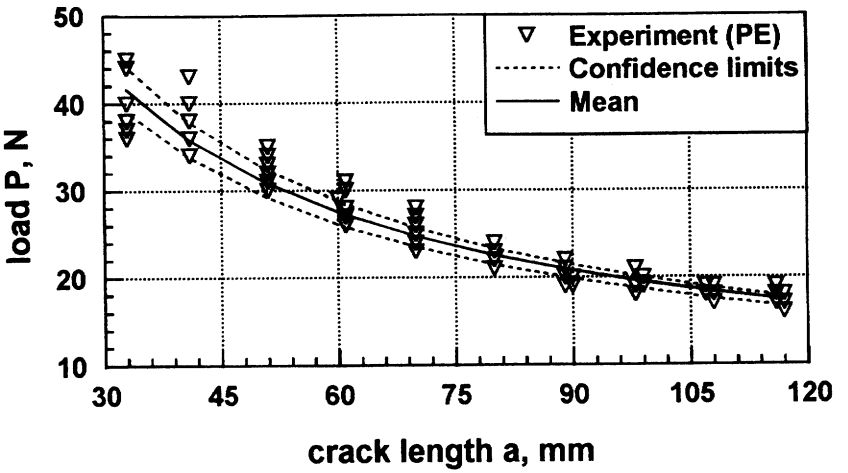

Figure 7. *Plot load* P *versus crack length* a *and the 95% confidence limits of the critical load in the DCB test for the composite PE.*

energy release rates $G_{IC}(a)$ or interlaminar fracture toughness has been performed. Firstly, the G_{IC} values obtained by the Berry method will be discussed. In this case the unknown quantity n in expression (8) is obtained from Equation (10) by a curve fit procedure. The related approximation of the experimental results for the composite with fiber surface treatment SI/EP is shown in Figure 8. It is seen that for this material $n = 2.99$has been found, which is close to the value 3 predicted by the classical beam theory. A similar equation of regression ($\lg C = 2.89 \lg a - 5.42$) was obtained for the composite with fiber surface treatment PE resulting in the parameter $n = 2.89$. Therefore, in the first step of the Berry method the parameters A_1 and n can be evaluated through Equation (10), and subsequently by using Equation (8) the critical energy release rates for each step of crack propagation can be calculated. The results based on the Berry method for the composites SI/EP and PE are presented in the Table 1.

The second method which has been used here in order to calculate the critical energy release rates G_{IC} is the compliance method. In this method formula (3) is applied and the analytical function $C = C(a)$ is obtained directly from the data of experiments through expression (10) and the coefficients, which for the composite SI/EP are presented in the caption of the Figure 9. By substituting the derivative of the compliance for a given crack length and the corresponding critical load P into formula (3) the critical energy release rates G_{IC} are calculated. The results obtained by the compliance method for the composites SI/EP and PE are also presented in the Table 1.

The third method of data reduction is based on the modified beam analysis. In

Table 1. Mode I energy release rates G_{IC} (a), calculated by six different methods.

Experiment			G_{IC} kJ/m^2					
P N	a mm	δ mm	Area Method Equation (2)	Berry Method Equation (8)	Modified Beam Analysis Equation (23)	Compl. Method Equation (3)	FEM Linear Analysis	FEM Non-linear Analysis
					SI/EP			
38.93	33.45	3.536	0.186	0.244	0.234	0.229	0.258	0.242
35.63	41.30	5.474	0.269	0.280	0.299	0.292	0.323	0.299
31.63	50.80	8.932	0.311	0.332	0.355	0.348	0.381	0.348
28.21	60.59	14.08	0.344	0.392	0.400	0.392	0.427	0.385
25.11	70.33	19.42	0.410	0.413	0.424	0.418	0.453	0.404
23.11	79.87	26.87	0.423	0.464	0.459	0.456	0.490	0.429
21.6	89.29	35.03	0.441	0.505	0.495	0.498	0.532	0.456
20.31	98.56	44.04	0.448	0.541	0.524	0.536	0.573	0.478
19.16	107.8	53.14	0.476	0.563	0.548	0.569	0.607	0.493
18.33	116.6	64.28	0.481	0.603	0.570	0.609	0.649	0.508
					PE			
38.41	33.43	4.280	0.157	0.285	0.245	0.246	0.259	0.243
36.98	40.88	6.173	0.294	0.323	0.340	0.334	0.365	0.336
32.56	50.75	10.09	0.323	0.374	0.405	0.390	0.415	0.378
28.43	60.57	14.39	0.400	0.390	0.438	0.415	0.446	0.401
24.83	70.28	20.09	0.414	0.410	0.447	0.420	0.458	0.407
22.06	79.87	26.88	0.428	0.429	0.451	0.422	0.459	0.404
20.30	89.31	34.85	0.454	0.458	0.472	0.441	0.482	0.417
19.14	98.53	44.31	0.453	0.498	0.501	0.472	0.524	0.441
18.13	107.7	53.90	0.453	0.525	0.527	0.501	0.560	0.459
17.40	116.6	64.48	0.489	0.556	0.553	0.532	0.602	0.477

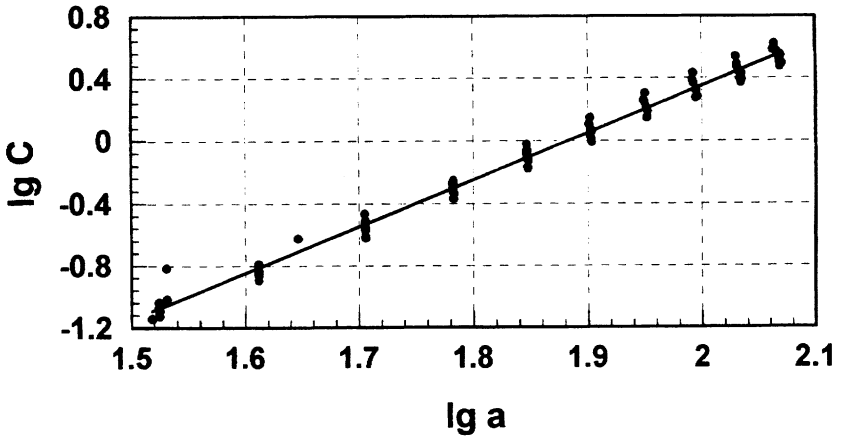

Figure 8. *Determination of the parameters* A_1 and n *by the least square method for the Berry method and the composite SI/EP (equation of regression lg* C = 2.99 *lg* a – 5.63*).*

order to obtain the correction coefficient χh, which is used in the modified beam analysis, directly from the experimental data the function of the corrected compliance C/N versus crack length by Equation (21) is required. The correction coefficients F and N are calculated by formulae (17) and (18) and the related data plot $(C/N)^{1/3}$ versus crack length a and the curve fit for the composite SI/EP are presented in Figure 9. In the same way the equation of regression for the composite PE can be obtained.

From Equation (21), where coefficients have been determined from the experimental data by the least square technique, the crack length correction term χh and the average value of longitudinal modulus E_1 can be calculated. The average values of the longitudinal modulus E_1 calculated from Equation (21) for both composites are presented in Table 2, where for comparison also the values obtained by tension tests [33] are presented. A good agreement between both results is found. For the composite SI/EP the value χh calculated from the equation of regression (see Figure 9) is to be negative. For the composite PE also the negative value of the correction term have been obtained. On the other hand the calculations of χh by the analytical formula (16) gives the following crack length correction values for the DCB test (h = 1.5 mm): χh = 2.34 mm (for the SI/EP composite) and χh = 2.28 mm (for the PE composite). These calculations were performed by using the longitudinal modulus E_1 obtained by the tension tests (see Table 3). It can be realized that these values of χh are rather small for both composites. Since the curve fit of the experimental data (see Figure 9) gives negative values of χh, the crack length correction term χh is assumed to be zero in further calculations.

Furthermore the longitudinal modulus E_1 can also be calculated from the DCB

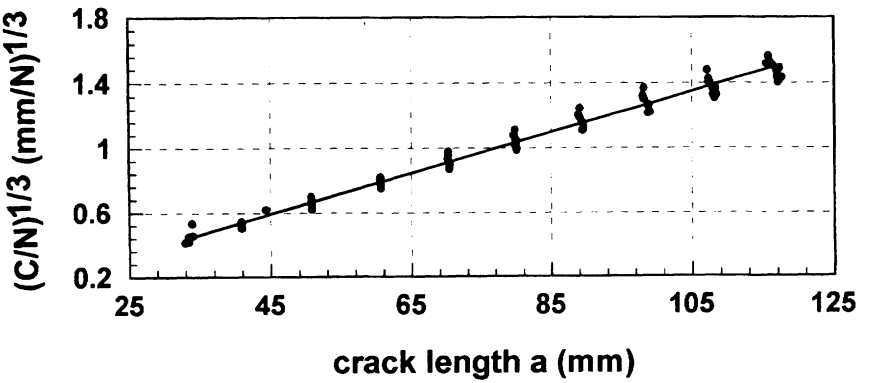

Figure 9. *Plot* $(C/N)^{1/3}$ *versus crack length a for the modified beam analysis and composite SI/EP (equation of regression lg* $(C/N)^{1/3} = 0.0134\ a - 0.142$*).*

test through formula (24). Then the longitudinal modulus E_1 is calculated for each crack length and the mean values (averaging for all steps of crack extension) of E_1 are presented in the last column of Table 2. A good agreement with the results form other methods of data reduction and also with the tension test results is observed.

Subsequently by using the data for E_1 in the formula (23) for each crack length the critical energy release rates G_{IC} can be calculated. The results obtained by the modified beam analysis for both composites are also presented in Table 1.

The fourth method of data reduction which is used in the present investigation is the area method. With this method the critical energy release rates G_{IC} can be calculated directly from the experimental data by using formulae (2). The correlated results for both composites again are presented in Table 1.

Finally, the DCB tests have been analyzed by the finite element method. Due to the large displacements to be realized during the experiments for longer crack length a geometric non-linear finite element analysis had to be performed. For comparison in Table 1 results of a linear finite element analysis also are presented. The unde-

Table 2. Evaluation of longitudinal modulus E_1 ***by different methods.***

	E_1 GPa		
Composite	Tension Test [33]	DCB Test, Compliance Fit Equation (21)	DCB Test, Mean Value Equation (24)
SI/EP	40.7	38.6	41.0
PE	39.7	37.8	38.0

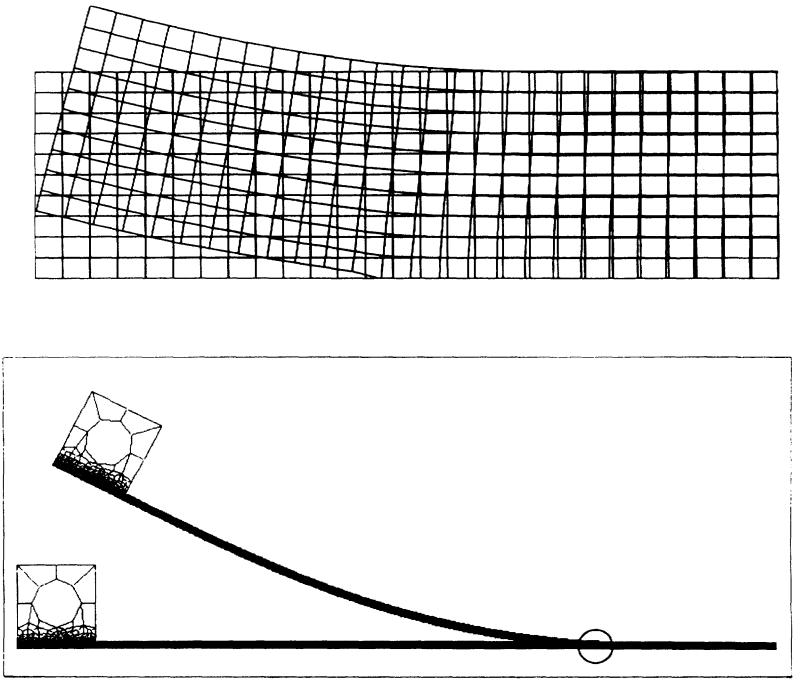

Figure 10. *Initial and deformed shape of the non-linear finite element model of the DCB test at crack length* a = *116.6 mm for the composite SI/EP.*

formed and deformed finite element meshes for the last step (a = 116.6 mm) of the non-linear finite element analysis is presented in the Figure 10.

From a detailed comparison of the results (see Table 1) it can be concluded that for crack lengths between 40 and 70 mm the critical energy release rates obtained from the DCB test with the different data reduction methods are in good agreement. However, conclusions that differences among the methods are statistically significant can be made only on the basis of statistical analysis of the experimental data. The 95% confidence limits of the critical energy release rates $G_{IC}(a)$ obtained by the linear and non-linear finite element analysis are presented in Figure 11. It is seen that for longer cracks (a > 70 mm) results for G_{IC} obtained by the geometric non-linear finite element analysis and by using the mean values of the critical loads are to be out of the confidence limits for G_{IC} obtained by the linear finite element analysis. For longer cracks (a > 70 mm) only the results obtained through the nonlinear finite element analysis and the area method are in good agreement (see Table 1), whereas all other data reduction methods deliver critical energy release rates that are too high by 15 to 30%. Results obtained by the modified beam analysis shows trend to decrease in comparison with the results obtained by the

conventional beam analysis. Also some differences for the crack initiation values in the first step of crack propagation are observed. In particular the crack initiation values obtained by the area method are lower than the values obtained by the methods based on the beam analysis and its modifications. Crack initiation values obtained by the finite element solution (linear and non-linear) are in good agreement with those obtained by the compliance method, conventional and modified beam analysis. All these values are to be in the 95% confidence limits of the G_{IC}^{init} obtained by the linear finite element analysis. So, it can be concluded that there are no statistically significant differences among the methods to calculate the crack initiation values G_{IC}^{init}. In the same time for longer cracks ($a > 70$ mm) there are statistically significant differences among the crack propagation values obtained by the geometric non-linear finite element analysis (also by the area method) and the values obtained by other data reduction methods (the Berry method, the compliance method and the modified beam analysis).

Furthermore it is of interest to analyze how the critical energy release rates depend on crack length. In Figure 11 it is seen that with crack growth a considerable increase of interlaminar fracture toughness was found and that stabilization of the crack resistance curves obtained by non-linear FE analysis and also by the area method (see Table 1) is observed only for rather long cracks. For the composite PE considerable increasing of the critical energy release rates at crack propagation is due to extensive fiber bridging, but for the composite SI/EP practically no fiber bridging was observed in the DCB tests.

From the detailed analysis of the results presented in Table 1, and also in Figure

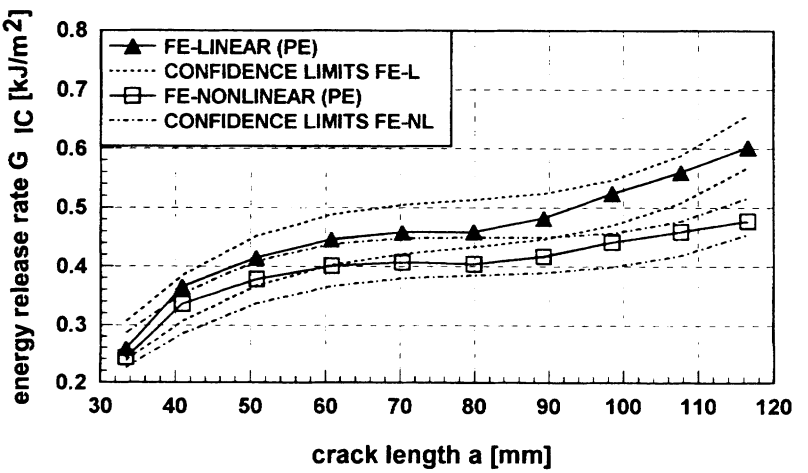

Figure 11. *The 95% confidence limits of* G_{IC} *obtained by the linear and non-linear finite element analysis for the composite PE.*

11 it is seen that critical energy release rates G_{IC}^{init} at crack initiation are much lower than critical energy release rates G_{IC}^{prop} at further crack propagation. For comparison the mean values of G_{IC}^{init} calculated as average of all values obtained by the 6 methods of data reduction applied in the present investigation have been calculated. In the same way the mean values of the energy release rates $G_{IC}^{s.s.prop}$ for steady state crack propagation can be obtained by averaging of G_{IC} for the last 2 steps of crack propagation (the last 2 rows for each material in Table 1). For the composite SI/EP the averaging gives the following results: $G_{IC}^{init} = 0.232\,\text{kJ/m}^2$ and $G_{IC}^{s.s.prop} = 0.557\,\text{kJ/m}^2$. The corresponding values for the composite PE are as follows: $G_{IC}^{init} = 0.238\,\text{kJ/m}^2$ and $G_{IC}^{s.s.prop} = 0.518\,\text{kJ/m}^2$.

Thus it is found that for both composites the Mode I critical energy release rates are of about the same value. However, by transverse tension tests it was obtained, that the transverse interlaminar strength in tension for the composite PE is about 3 times lower than for the composite SI/EP. The higher values of G_{IC} that are found here for the composite PE can be explained by extensive fiber bridging and pull-out in the DCB test, whereas for the composite SI/EP practically no fiber bridging and pull-out was observed in the DCB tests. Therefore, in the case of fiber bridging (composite PE) the crack surface on the micro level is much greater than the crack macro surface $A = b \times a$, which has been considered for the calculation of G_{IC}.

5.2 Mode II ENF Test

For the Mode II ENF test (see Figure 4) 4 specimens for each type of composite SI/EP and PE were used. Before the tests Mode I precracks of length from 4 to 10 mm were introduced and since in the ENF test the crack growth is unstable, only crack initiation values G_{IIC}^{init} can be obtained. In Table 3 the mean values of experimental data for the critical load and displacement are presented.

For the ENF test the crack length correction term χh calculated according to formula (16) is $\chi h = 0.98$ mm for the composite SI/EP and $\chi h = 0.95$ mm for the

Table 3. Mode II ENF test critical energy release rates calculated without friction ($\mu = 0$) and with friction ($\mu = 0.7$) along the crack surfaces.

	Experiment		Beam Analysis Equation (12)	FEM Linear Analysis ($\mu = 0$)			FEM Linear Analysis ($\mu = 0.7$)	
Composite	P N	δ mm	G_{IIC}^{init} kJ/m²	δ mm	G_{IIC}^{init} kJ/m²	G_{TC}^{init} kJ/m²	δ mm	G_{IIC}^{init} kJ/m²
SI/EP	870	4.87	2.070	4.18	1.873	1.893	4.14	1.741
PE	540	3.18	0.839	2.67	0.744	0.751	2.64	0.690

composite PE. Since these values are rather small, $\chi h = 0$ mm is assumed again. Also the displacements are rather small (see Table 3) and so the correction factor F in formula (19), which takes large displacements into account, is assumed to be unity ($F = 1$), and, therefore, the data reduction can be carried out by linear beam analysis according to formula (12). It should be noted that in the ENF test (see Figure 4) contact and friction along the crack surfaces will occur adjacent to the support. In order to estimate the influence of friction in the ENF test the geometric linear finite element analysis with different coefficients of friction μ have been performed. The corresponding results are presented in Table 3. In these calculations the finite element analysis takes contact, friction and the related energy dissipation at the crack surfaces into account in the same way as for the cross-ply laminates [41]. The analysis reveals that due to the energy dissipated in friction along the crack surfaces the critical energy release rates G_{IIC}^{init} at the crack tip are lower for about 15% in comparison with the linear beam analysis without taking friction into account. The frictional work W^F [see Equation (32)] is about 6% ($\mu = 0.7$) of the total potential energy.

In order to compare the results obtained by the local method [VCCI method, Equation (34)] and by the global method [Equation (33)] in Table 3 also the total critical energy release rates G_{TC}^{init} for crack initiation are presented for $\mu = 0$. Since the Mode I energy release rate for the ENF test practically is equal to zero, the Mode II critical energy release rate G_{IIC}^{init} must be equal to the total critical energy release rate G_{TC}^{init}. It is seen that the results obtained by the local and the global methods are in good agreement.

From the comparison of the results for the two different materials it is seen that the Mode II critical energy release rate G_{IIC}^{init} for the composite SI/EP is about 2.5 times higher than for the composite PE. This result is in good agreement with the value of the transverse interlaminar strength in tension, which is about three times higher for the composite SI/PE [33]. For both composites Mode II cracks propagate without fiber bridging and, therefore, the value G_{IIC}^{init} indirectly characterizes the fiber/matrix adhesion properties. It should be mentioned that for the ENF test the area and the compliance method cannot be employed, since the crack growth in the experiments is unstable so that only the first critical load and the corresponding displacements can be measured.

5.3 Mixed Mode I/II MMF Test

For the mixed Mode I/II MMF experiment (see Figure 5) also 4 specimens for each type of the composites were tested. Before the test Mode I precracks of length from 3 to 5 mm were introduced. In the case of the MMF test again stable crack growth was found. In the experiments four steps of crack propagation were obtained with a crack extension for each step of about $\Delta a = 5$ mm. In the Table 4 the mean values of experimental data for the critical load and displacement are pre-

Table 4. Total G_{TC} and separated G_{IC} and G_{IIC} critical energy release rates calculated from the MMF test.

Experiment			Area Method Equation (2)	Beam Analysis Equation (28)	FEM Linear Analysis				
a mm	*P* N	δ mm	G_{TC} kJ/m^2	G_{TC} kJ/m^2	δ mm	G_{IC} kJ/m^2	G_{IIC} kJ/m^2	G_{TC} kJ/m^2	G_I / G_{II}
				SI/EP					
19	256.6	1.780	0.383	0.456	1.550	0.244	0.163	0.407	1.49
24	206.2	1.982	0.462	0.498	1.655	0.243	0.166	0.409	1.46
29	170.2	2.307	0.474	0.505	1.861	0.236	0.163	0.399	1.44
34	145.8	2.925	0.440	0.546	2.185	0.234	0.164	0.398	1.42
				PE					
19	224.5	1.705	–	0.384	1.402	0.192	0.128	0.320	1.50
24	220.7	1.980	–	0.525	1.824	0.286	0.195	0.482	1.46
29	207.5	2.260	–	0.602	2.336	0.360	0.250	0.611	1.44
34	184.8	2.745	–	0.648	2.852	0.388	0.271	0.659	1.43

sented. The data reduction for the MMF test has been performed by the beam analysis and by the linear finite element approach. In the case of linear beam analysis the total energy release rate G_{TC} is calculated by formula (14). The results of the calculations are presented in Table 4. The separated Mode I and Mode II critical energy release rates G_{IC} and G_{IIC} can be calculated by formula (15), which is based on linear beam theory, or by the FE analysis, which gives slightly higher mixed mode ratios (see last column in Table 4) and some dependence on crack length.

It should be noted that due to stable crack growth in the MMF test the data reduction can also be performed by the compliance method and by the area method. For the composite SI/EP the mean values (mean of all four specimens) of the total energy release rates obtained by the area method also are presented in Table 4. There are some differences, but in general the results from different approaches are in rather good agreement.

From a detailed analysis of the results presented in Table 4 it is seen that in the values of the critical energy release rates for crack initiation there are some differences. For the composite PE the crack initiation value is lower ($G_{TC}^{init} = 0.352\,\mathrm{kJ/m^2}$) than for the composite SI/EP ($G_{TC}^{init} = 0.405\,\mathrm{kJ/m^2}$). These values are calculated as mean values obtained by three different methods (area method, linear beam analysis and linear FE analysis) for the composite SI/EP and by the two methods (linear beam analysis and linear FE analysis) for the composite

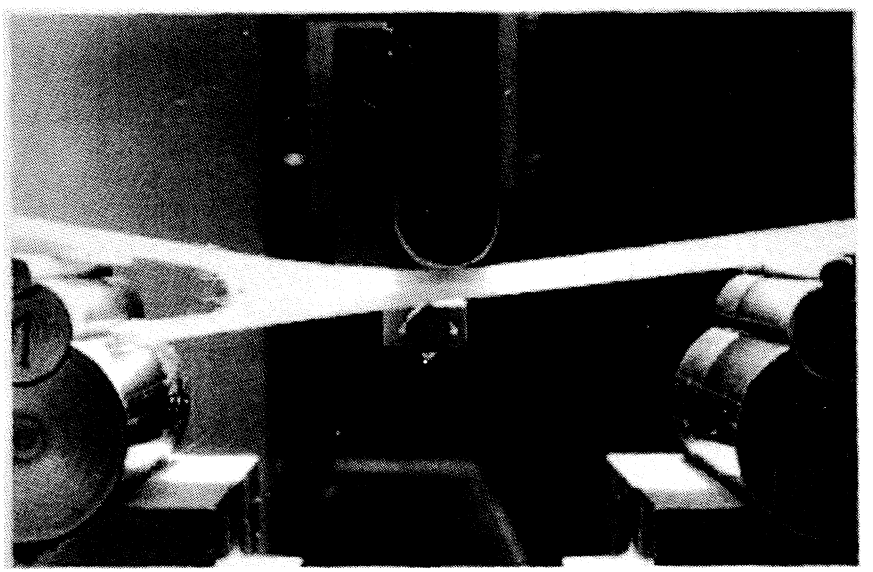

Figure 12. *Mixed Mode I/II MMF test for the composite PE with fiber bridging between the delamination crack surfaces.*

PE. Similarly as in DCB test for the composite PE in the MMF test an extensive fiber bridging and pull-out has been observed with crack extension (see Figure 12). On the other hand in the MMF test for the composite SI/EP fiber bridging with crack extension has practically not been observed. Therefore, due to fiber bridging the critical energy release rates G_{TC}^{prop} for crack propagation is even higher for the composite PE than for the composite SI/EP. The critical energy release rates $G_{TC}^{s.s.prop}$ for steady state crack propagation are calculated as average of values for the last two steps of crack extension $a = 25$ mm and $a = 34$ mm. The calculated mean values of the total critical energy release rates obtained by the methods under consideration here are as follows: $G_{TC}^{s.s.prop} = 0.460\,\mathrm{kJ/m^2}$ (composite SI/EP) and $G_{TC}^{s.s.prop} = 0.630\,\mathrm{kJ/m^2}$ (composite PE).

6. CONCLUSIONS

Mode I, Mode II and mixed Mode I/II delamination crack propagation experiments have been performed. Two types of fiber surface treatments have been investigated. A summary of the results of the interlaminar fracture toughness for both composites is given in Table 5, where the mean values calculated as average of values obtained by different methods are presented. The Mode I critical energy release rates for crack initiation are about of the same value for both composites. The Mode II critical energy release rate for crack initiation of the composite SI/EP is about 2.5 times higher than for the composite PE. This result is in good agreement with the interlaminar transverse strength in tension, which for the composite SI/EP is about 3 times higher. In the case of mixed Mode I/II loading the interlaminar crack propagates similarly as the Mode I crack.

From comparison of the critical energy release rates obtained by using different methods of data reduction it can be concluded that there are no statistically significant differences for the Mode I crack initiation values G_{IC}^{init}. The critical energy release rates of the crack initiation G_{IC}^{init} can be calculated by all methods considered here. For the longer cracks there are statistically significant differences of the results for G_{IC} obtained by the geometric non-linear finite element analysis and by the area method in comparison with other methods. For the longer cracks the area

Table 5. Mean values of interlaminar fracture toughness obtained by all methods of data reduction used in the present investigation.

	DCB Test Mode I		ENF Test Mode II	MMF Test Mixed Mode I/II	
Composite	G_{IC}^{init} kJ/m^2	$G_{IC}^{s.s.prop}$ kJ/m^2	G_{IIC}^{init} kJ/m^2	G_{TC}^{init} kJ/m^2	$G_{TC}^{s.s.prop}$ kJ/m^2
SI/EP	0.232	0.557	1.890	0.405	0.460
PE	0.238	0.518	0.758	0.352	0.630

method or non-linear finite element analysis must be used. The critical energy release rates obtained by the compliance method, by the Berry method and by the linear finite element analysis for the longer cracks are to be overestimated. In the ENF tests the Mode II critical energy release rates obtained by the finite element analysis taking into account contact and friction along the crack surfaces are about 15% lower than those obtained on the basis of conventional beam analysis. The frictional work in the ENF test is about 6% (for the frictional coefficient $\mu = 0.7$) of the total potential energy of the specimen.

ACKNOWLEDGEMENTS

This study was performed in the framework of a project on design of interfaces of glass fiber reinforced composites. The project is performed in cooperation between the universities of Riga, Kassel and Paderborn. The authors gratefully acknowledge the financial support by VW Foundation (Hannover, Germany) through grant I/70 665. The authors also would like to thank Dr. H. Frenzel at the Institute of Polymer Research (Dresden, Germany) for preparing and providing the glass fibers with different surface treatments.

REFERENCES

1. Piggott, M. R. 1992. "Interface Properties and Their Influence of Fibre-Reinforced Polymers," in T. Vigo and B. Kinzig (eds.), *Composite Applications. The Role of Matrix, Fibre and Interface,* New York: VCH Publishers, pp. 221–266.
2. Sela, N. and O. Ishai. 1989. "Interlaminar Fracture Toughness and Toughening of Laminated Composite Materials, A Review," *Composites,* 20:423–435.
3. Albertsen, H., J. Ivens, P. Peters, M. Wevers and I. Verpoest. 1995. "Interlaminar Fracture Toughness of CFRP Influenced by Fibre Surface Treatment: Part 1. Experimental Results," *Comp. Sci. Technol.,* 54:133–145.
4. Chai, H. 1986. "On the Correlation between the Mode I Failure of Adhesive Joints and Laminated Composites," *Eng. Fract. Mech.,* 24:413–431.
5. Keary, P. E., B. L. Ilcewicz, C. Shar and J. Trostle. 1985. "Mode I Interlaminar Fracture Toughness of Composites Using Slender Double Cantilevered Beam Specimens," *J. Comp. Mater.,* 19:154–177.
6. Zhao, S., M. Gädke and R. Prinz. 1995. "Mixed-Mode Delamination Behavior of Carbon/Epoxy Composites," *J. Reinf. Plast. and Comp.,* 14:804–826.
7. Hashemi, S., A. J. Kinloch and G. Williams. 1990. "Mechanics and Mechanisms of Delamination in a Poly(ether sulphone)-Fibre Composite," *Comp. Sci. Technol.,* 37:429–462.
8. Hashemi, S., A. J. Kinloch and G. Williams. 1990. "The Analysis of Interlaminar Fracture in Uniaxial Fibre-Polymer Composites," *Proc. R. Soc. Lond.,* A427:173–199.
9. Yeoung, P. and L. J. Broutman. 1978. "The Effect of Glass-Resin Interface Strength on the Impact Strength of Fiber Reinforced Plastics," *Polymer Eng. and Sci.,* 18:62–72.
10. Davidson, B. D., R. Krüger and M. König. 1995. "Three-Dimensional Analysis of Center-Delaminated Unidirectional and Multidirectional Single-Leg Bending Specimens," *Comp. Sci. Technol.,* 54:385–394.

11. Davies, P., C. Moulin and H. H. Kausch. 1990. "Measurement of G_{IC} and G_{IIC} in Carbon/Epoxy Composites," *Comp. Sci. Technol.*, 39:193–205.

12. Carlsson, L. A., J. W. Gillespie and R. B. Pipes, Jr. 1986. "On the Analysis and Design of the End Notched Flexure (ENF) Specimen for Mode II Testing," *J. Comp. Mater.*, 20:594–605.

13. Reeder, J. R. and J. H. Crews, Jr. 1990. "Mixed-Mode Bending Method for Delamination Testing," *AIAA J.*, 28:1270–1276.

14. Hashemi, S., A. J. Kinloch and G. Williams. 1990. "The Effects of Geometry, Rate and Temperature on the Mode I, Mode II and Mixed-Mode I/II Interlaminar Fracture of Carbon-Fibre/Poly(ether-ether ketone) Composites," *J. Comp. Mater.*, 24:918–956.

15. Davies, P. et al. 1992. "Round-Robin Interlaminar Fracture Testing of Carbon-Fibre-Reinforced Epoxy and PEEK Composites," *Comp. Sci. Technol.*, 42:129–136.

16. Madhukar, M. S. and L. T. Drzal. 1992. "Fibre-Matrix Adhesion and Its Effect on Composite Mechanical Properties," IV. Mode I and Mode II Fracture Toughness of Graphite/Epoxy Composites, *J. Comp. Mater.*, 26:936–968.

17. Ratwani, M. M. and R. B. Deo. 1986. "Resistance Curve Approach to Composite Materials Characterization," in *Fracture Mechanics, Vol. 17. 17th National Symposium on Fracture Mechanics, Albany (New York), 7–9 August, 1984. American Society for Testing of Materials, ASTM STP 905,* Philadelphia, pp. 108–123.

18. Hashemi, S., A. J. Kinloch and G. Williams. 1989. "Corrections Needed in Double-Cantilever Beam Test for Assessing the Interlaminar Failure of Fibre-Composites," *J. Materials Sci. Letters,* 8:125–129.

19. Davies, P. and M. L. Benzeggah. 1989. "Interlaminar Mode-I Fracture Testing," in R. B. Pipes (ed.), *Application of Fracture Mechanics to Composite Materials, Vol. 6,* K. Friedrich (ed.), *Composite Materials Series,* Amsterdam: Elsevier, pp. 81–112.

20. Carlsson, L. A. and J. W. Gillespie, Jr. 1989. "Mode-II Interlaminar Fracture of Composites," in R. B. Pipes (series ed.), *Application of Fracture Mechanics to Composite Materials, Vol. 6,* K. Friedrich (ed.), *Composite Materials Series, Amsterdam, Elsevier,* pp. 113–157.

21. Zhou, J. and T. He. 1994. "On the Analysis of End-Notched Flexure Specimen for Measuring Mode II Fracture Toughness of Composite Materials," *Comp. Sci. Technol.*, 50:209–213.

22. Maikuma, H., J. W. Gillespie, Jr. and J. M. Whitney. 1989. Analysis and Experimental Characterization of the Center Notch Flexural Test Specimen for Mode II Interlaminar Fracture," *J. Comp. Mater.*, 23:756–786.

23. O'Brien, T. K. 1984. "Mixed-Mode Strain Energy Release Rate Effects on the Edge Delamination of Composites," in *Effects of Defects in Composite Materials, American Society for Testing of Materials, ASTM STP 836,* Philadelphia, pp. 125–142.

24. Kinloch, A. J., Y. Wang, J. G. Williams and P. Yayla. 1993. "The Mixed Mode Delamination of Fibre Composite Materials," *Comp. Sci. Technol.*, 47:225–237.

25. Wang, Y. and J. G. Williams. 1992. "Corrections for Mode II Fracture Toughness Specimens of Composite Materials," *Comp. Sci. Technol.*, 43:129–136.

26. Drzal, L. T., M. J. Rich and P. F. Lloyd. 1982. "Adhesion of Graphite Fibres to Epoxy Matrices: 1. The Role of Fibre Surface Treatment," *J. Adhesion,* 16:1–30.

27. Gutowski, W. S., E. R. Pankevicius and D. Y. Wu. 1993. "Controlled Interfaces of Ultra-High Modulus of Polyethylene and Aramid Fibres for Advanced Composites," in *Proc. Int. Conf. Interfaces II,* CAMT, Ballart, Australia.

28. Drzal, L. T. 1986."The Interphase in Epoxy Composites," *Advances in Polymer Science,* 75:1–31.

29. Plueddemann, E. P. 1982. *Silane Coupling Agents,* New York: Plenum Press.

30. Plueddemann, E. P. 1992. "Reminiscing on Silane Coupling Agents," in *Silane and Other Coupling Agents,* K. L. Mittal (ed.), The Netherlands: VSP BV, Utrecht, pp. 3–19.

31. Ishida, H. A. 1986. "Review of a Recent Progress in the Studies of Molecular and Microstructure of Coupling Agents and Their Functions in Composites, Coatings and Adhesive Joints," *Polymer Composites,* 5:101–123.
32. Bledzki, A. K., G. Wacker and H. Frenzel. 1993. "Effect of Surface Treated Glass Fibres on the Dynamic Behaviour of Fibre-Reinforced Composites," *Mechanics of Composite Materials,* 29:585–591.
33. Wacker, G. 1996. "Experimentell Gestützte Identifikation Ausgewählter Eigenschaften Glasfaserverstärkter Epoxidharze unter Berücksichtigung der Grenzschicht," PhD Dissertation, University of Kassel, Kassel, Germany, (in German).
34. Gibson, R. F. 1994. *Principles of Composite Material Mechanics,* McGraw-Hill.
35. Hojo, M., K. Kageyama and K. Tanaka. 1995. "Prestandardization Study on Mode I Interlaminar Fracture Toughness Test for CFRP in Japan," *Composites,* 26:243–255.
36. Broek, D. 1986. *Elementary Engineering Fracture Mechanics,* 4th Ed., Dordrecht, The Netherlands: Martinus Nijhoff Publishers.
37. Berry, J. P. 1963. "Determination of Fracture Surface Energies by the Cleavage Technique," *J. Appl. Physics,* 34:62–68.
38. Hibbitt, Karlson and Sorensen, Inc. 1993. *ABAQUS User's Manual, Version 5.3,* Providence Rhode Island.
39. Rybicki, E. F. and M. F. Kanninen. 1977. "A Finite Element Calculation of Stress Intensity Factors by Modified Crack Closure Integral," *Engng. Fracture Mech.,* 9:931–938.
40. Buchholz, F.-G. 1984. "Improved Formulae for the Finite Element Calculation of the Strain Energy Release Rate by Modified Crack Closure Integral Method," in J. Robinson (ed.), *Accuracy, Reliability and Training in FEM Technology, Proc. of the 4th World Congr. and Exib. on Finite Element Methods, Interlaken, Switzerland, September 1984,* Dorset: Robinson and Associates, pp. 650–659.
41. Rikards, R., F.-G. Buchholz and H. Wang. 1995. "Finite Element Analysis of Delamination Cracks in Bending of Cross-Ply Laminates," *Mech. Comp. Mater. and Struct.,* 2:281–294.